ORIGINAL PAPER

Feng-Yun Wang · Soofin Cheng · Chen-Hung Chung
Ben-Zu Wan

Y$_2$O$_3$ and MgO co-doped ceria based electrolytes

Abstract Electrolytes of $Ce_{1-x-y}Y_xMg_yO_{2-0.5x-y}$ were pre-
pared with citrate method and were characterized by
inductively coupled plasma-atomic emission spectrome-
try, energy dispersive spectrometry, powder X-ray dif-
fraction, and impedance spectroscopy. The effect of
composition on the structure, conductivity, and stability
of the electrolytes were investigated. When $0 \leq x \leq$ about
0.2 and $0 \leq y \leq$ about 0.05, the electrolytes were all single
phase materials of ceria-based solid solution. However,
when y > about 0.05, the electrolytes became two-phase
materials, Y^{3+} and Mg^{2+} co-doped ceria-based solid
solution and free MgO. The sample with nominal com-
position of $Ce_{0.815}Y_{0.065}Mg_{0.12}O_{2-d}$ showed ionic con-
ductivity at 973 K close to or even a little higher than that
of similarly prepared $Ce_{0.9}Gd_{0.1}O_{1.95}$, but had lower cost
of raw materials and a little better stability in reducing
atmosphere. The existing of free MgO improved the sta-
bility of the electrolytes in reducing atmosphere, but too
much free MgO reduced the conductivity.

Keywords Solid electrolyte · Co-doped ceria ·
MgO · Y$_2$O$_3$ · Conductivity

Introduction

Doped ceria systems have a long history of investiga-
tion as potential materials for oxide ion conducting

F.-Y. Wang · S. Cheng (✉) · C.-H. Chung
Department of Chemistry, National Taiwan University,
Taipei, 106, Taiwan
E-mail: Chem1031@ntu.edu.tw
Tel.: +886-2-23638017
Fax: +886-2-23636359

F.-Y. Wang (✉)
Department of Chemistry, Foshan University,
Foshan, 528000, P.R.China
E-mail: copking@126.com

B.-Z. Wan
Department of Chemical Engineering,
National Taiwan University, Taipei, 106, Taiwan

electrolytes. While the materials have found applica-
tions as oxygen sensor [1], oxygen concentrator cell [2]
etc., the most attractive application would be as the
electrolytes of intermediate temperature solid oxide
fuel cells (ITSOFC) [3]. Although a wide variety of
dopants have been shown to be effective in increasing
oxide ionic conductivity of doped ceria, alkaline earth
and rare earth cations, especially Gd^{3+} and Sm^{3+} are
considered preferred dopants. The doped ceria with
either Gd^{3+} or Sm^{3+} shows ionic conductivity much
higher than any reported yttria-stabilized zirconia
(YSZ) electrolyte in intermediate temperature (IT)
range (773∼973 K). However, at low oxygen partial
pressures with associated anodic conditions, the Ce^{4+}
ion of the electrolytes can be partially reduced to Ce^{3+}
[4]. As a result, electronic conduction is developed,
which lessens the power output of fuel cells. To solve
this problem and/or further improve the ionic con-
ductivity, some co-doped ceria were studied. For
example, $Ce_{0.8}Gd_{0.2-x}Pr_xO_{2-d}$ was found a little better
than $Ce_{0.8}Gd_{0.2}O_{2-d}$ in both anti-reduction and ionic
conductivity at 973 K [5]. $Ce_{0.685}Gd_{0.274}Mg_{0.041}O_{2-d}$
was found a little better than $Ce_{0.685}Gd_{0.315}O_{2-d}$ in
ionic conductivity at 996 K [6]. Although some pro-
gresses have been made, the problem remains.

In addition to this problem, doped ceria being re-
ported so far are still expensive. No matter singly doped
or multiply doped ceria, the dopants were usually chosen
from either rare earth cations or alkaline earth cations,
or both of them, and the total content of the rare earth
cations (including Ce^{4+}) was usually more than
90 mol%. Since rare earth materials are expensive, the
cost of raw materials of the doped ceria being reported
so far are still high.

Therefore, it is necessary to study ceria-based elec-
trolytes for better stability in reduction atmosphere,
lower cost of raw materials, and even higher ionic con-
ductivity. One possible way might be co-doping ceria
with cheaper dopants, such as Mg^{2+} and Y^{3+} or mak-
ing composite materials with the co-doped ceria and free
MgO. Although Mg^{2+} and Y^{3+}, among other alkaline

earth cations and rare earth cations, have the size most close to that of Ce^{4+} ion, and both MgO and Y_2O_3 are relatively cheap and stable, there is still a lack of systematic study on Y^{3+} and Mg^{2+} co-doped ceria materials and their composite materials with free MgO.

In this work, Y^{3+} and Mg^{2+} co-doped ceria and its composite materials with MgO were prepared and characterized. The effect of composition on the structure, conductivity, and stability of the electrolytes were investigated.

Materials and methods

Sample preparation

The starting materials were the nitrate salts of reagent grade (Acros) and used as purchased. The aqueous solutions of each metal ions of Y^{3+}, Ce^{4+}, and Mg^{2+} were prepared by dissolving the nitrate salt in distilled water and diluting them to desired concentrations. An aqueous solution of citric acid (CA) and polyethylene glycol (PEG) in a weight ratio of $CA/PEG = 60$ was also prepared and termed as CP solution. According to the composition ($Ce_{1-x-y}Y_xMg_yO_{2-d}$, wherein $0 \leq x \leq 0.765$, $0 \leq y \leq 0.80$) of the electrolyte samples, different volumes of metal ion solutions were taken and mixed in a beaker. Then, CP solution was added in the beaker until the molar number of citric acid was equal to the total number of the metal ions in the beaker. The mixed solution was evaporated under constant stirring at 353 K until the solution became gelled. The gel was dried at 378 K, ground and calcined in air at 973 K for 4 h, and then ground again to form calcined powder. The powder was uniaxially pressed under 750 MPa into green pellets using a stainless steel die with 13 mm diameter. The green pellets were then sintered in air at 1,773 K for 14 h with a heating rate of 1 K/min to form dense pellets (simplified as pellet hereafter).

For comparison, the pellet, having composition of $Ce_{0.9}Gd_{0.1}O_{1.95}$(CGO), was also prepared by a process analogous to the process described above.

Sample characterization

The crystal phases of the powder and the pellet (ground to powder again for measurement) samples were identified at room temperature using a PANalytical X-ray diffractometer (XRD) (45 kV, 40 mA, Cu K α radiation). The compositions of the pellet samples were analyzed using an inductively coupled plasma-atomic emission spectrometer (ICP-AES) (Jarrell-Ash, ICAP9000) and an energy dispersive spectrometer (EDS) (Hitachi S-2400 scanning electron microscope, Kevex Delta class 80000 EDS). Scanning electron microscopy (SEM) analysis of the cross-section of the pellets was conducted on a Hitachi S-2400 electron microscope.

Conductivity measurement

For conductivity measurement, Ag paste was brushed onto both sides of the pellet, then sintered at 1,073 K for 30 min to form Ag electrodes. Pt leads were attached to the electrodes using Ag paste and were sintered again at 1,073 K for 30 min. Impedance was measured using the two-probe method with an Autolab Impedance Analyzer (30 mV, 1 MHz–0.01 Hz). The measurements were taken at constant temperature within 473–973 K and in air (25 sccm). Prior to data collection at each temperature, the system was kept at the constant temperature and in given gas flow for 30 min. The conductivity data were obtained from the impedance plots by using the same method as that described in details in the literature [7]. In the following context, the word "conductivity" is used to represent the total conductivity (S_t) of grain and grain boundary.

The stability of electrolytes in 10% H_2/N_2 was tested at 973 K by monitoring the change of conductivity with time in the given atmosphere.

It has been documented that the main contribution of the conductivity of ceria-based compounds in air is oxide ionic conductivity (>99.5%) and that from electronic conductivity is negligible [3, 7]. In this study, the conductivity measured in air was treated as the oxide ionic conductivity only.

Results and discussion

Compositions

The compositions of pellet samples were analyzed with EDS and ICP. For ICP analysis, the samples were ground to powder form and dissolved in the mixed solution of hydrofluoric acid and nitric acid. The results of two typical samples were listed in Table 1. The compositions analyzed by both techniques were close to

Table 1 Chemical compositions of the pellet samples

Sample	Ce:Gd:Y:Mg atomic ratio		
	Designed	EDS	ICP
$Ce_{0.90}Gd_{0.10}O_{1.95}$	0.9:0.1:0:0	0.907:0.093:0:0	0.906:0.094:0:0
$Ce_{0.450}Y_{0.050}Mg_{0.500}O_{1.475}$	0.45:0:0.05:0.5	0.490:0:0.047:0.463	0.411:0:0.049:0.540

the nominal values, indicating that the effect of multi-step preparation, which included the high temperature sintering, on the compositions of the pellet samples is negligible. Therefore, it is reliable to use the nominal composition data of the pellet samples directly.

Crystal structure

For all the electrolyte samples of this work, it was found that calcined samples showed the same XRD patterns as the sintered samples of the same compositions, except that the XRD peaks were less sharp for the former than for the latter. This implies that the sintering process just caused the increase of crystal size and the increase of pellet compaction.
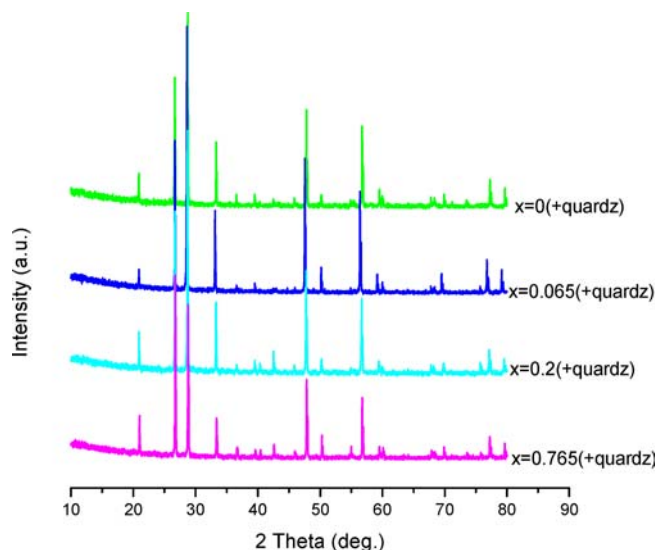
Figure 1 shows the XRD patterns of pellet samples with the nominal composition of $Ce_{0.935-y}Y_{0.065}Mg_yO_{1.9675-y}$, wherein $0 \leq y \leq 0.80$. Here, quartz was used as inner standard. It seems that all the samples have the same XRD patterns as pure ceria. However, when the XRD patterns were amplified to a sufficient extent, a minor peak of free MgO at about 43° was observed for the samples with $y > 0.05$. This result indicates that the samples with $y < 0.05$ are single-phase materials of ceria-based solid solution; whereas, the samples with $y > 0.05$ are two phase materials, Y and Mg codoped ceria solid solution and free MgO. Similarly, it has been reported in

Fig. 1 XRD patterns of the pellet samples with nominal composition of $Ce_{0.935-y}Y_{0.065}Mg_yO_{1.9675-y}$, wherein $0 \leq y \leq 0.80$, with quartz as inner standard and Cu as target
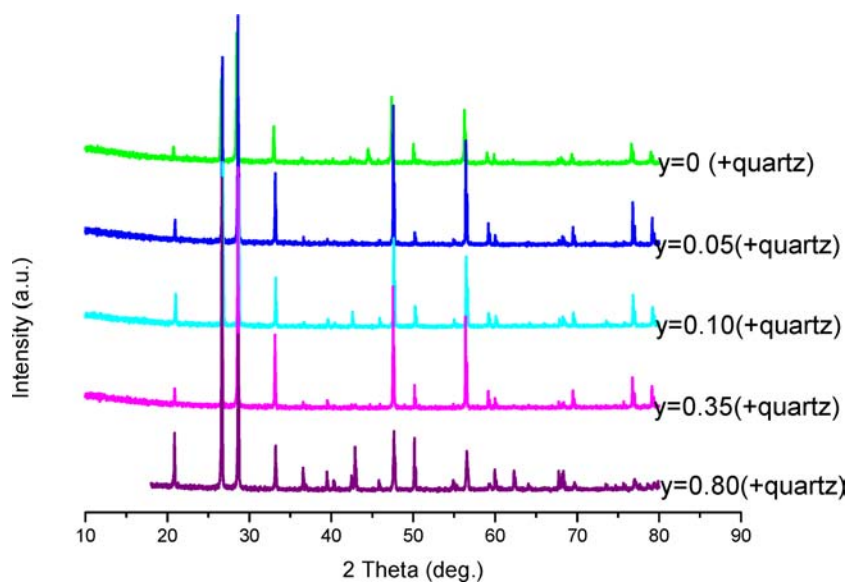
Fig. 2 Dependence of the lattice constant of the ceria-based solid solution phase on the total Mg content (y) of the pellet samples with nominal composition of $Ce_{0.935-y}Y_{0.065}Mg_yO_{1.9675-y}$
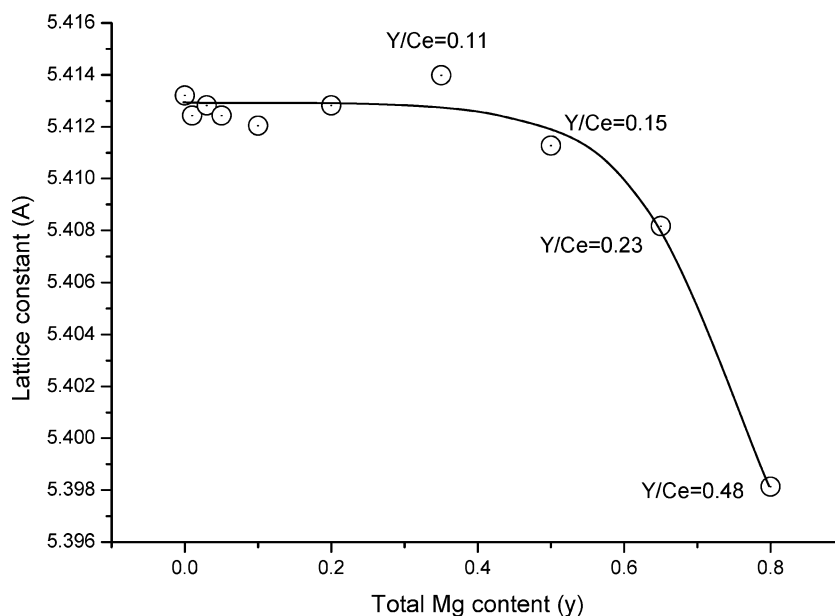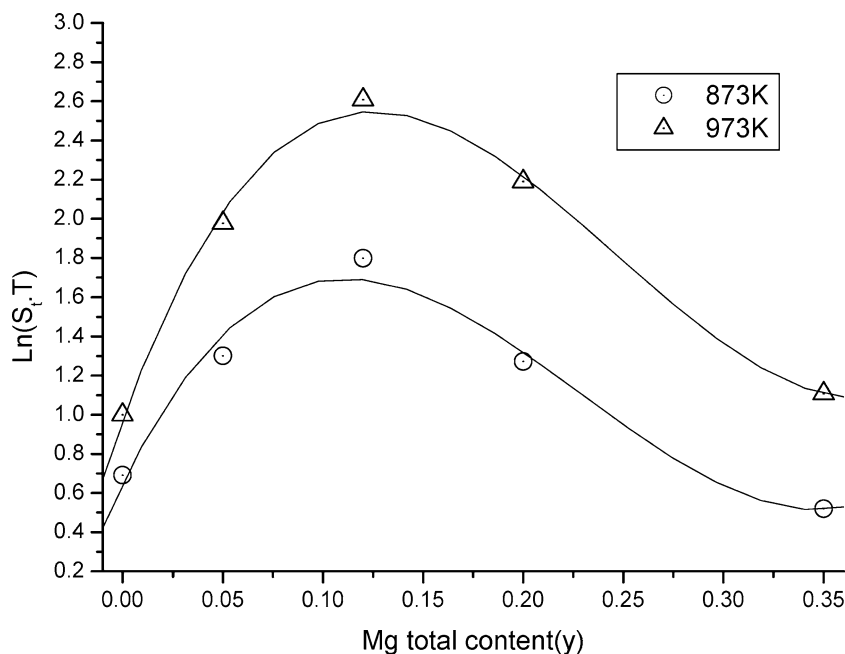
Fig. 3 XRD patterns of the pellet samples with nominal composition of $Ce_{0.6175-0.5x}Y_xMg_{0.3825-0.5x}O_{1.6175}$, wherein $x = 0\sim0.765$, with quartz as inner standard, and Cu as target

the literature [3] that the solubility of MgO in ceria was about 2 mol%.

Figure 2 shows the dependence of lattice constant of ceria-based solid solution phase on the total Mg content (y) of the pellet samples with the nominal composition of $Ce_{0.935-y}Y_{0.065}Mg_yO_{1.9675-y}$, wherein $0 \leq y \leq 0.80$. With y increasing, the lattice constant decreased weakly in the range of $y < 0.5$, but dramatically in the range of $y > 0.5$. It has been reported [3] that the lattice constant of Mg doped CeO_2 hardly changed with Mg content in the range of 0–50 mol%, and that the lattice constant of Y doped CeO_2 apparently decreased with the increase of Y

content. Therefore, for our work, the increase of y in the range of $y < 0.5$ did not apparently affect the lattice constant just because Mg has a very little solubility in CeO_2. However, when $y > 0.5$, the large increase of y caused a large increase of Y/Ce ratio, and in turn caused an apparent decrease of the lattice constant.

In order to investigate the effect of Y content (x) and at the same time to avoid the effect of oxygen content, a set of samples were prepared with the nominal composition of $Ce_{0.618-0.5x}Y_xMg_{0.382-0.5x}O_{1.618}$, wherein $0 \leq x \leq 0.765$. Figure 3 shows the XRD patterns of these pellet samples with quartz as inner standard. It seems that all the samples had the XRD patterns similar to that of pure ceria. However, when the XRD patterns were amplified to a sufficient extent, free MgO peak (at about 43°) was observed for the samples with $x = 0$–0.2, but no Y_2O_3 peak was observed for the samples with $x = 0.765$. This result indicates that the samples with $x = 0$–0.2 are two-phase materials of free MgO and ceria based solid solution. Since the solubility of Y_2O_3 in CeO_2 has been reported to be less than 58 mol% [3], the sample with $x = 0.765$ might also be a two-phase material of Y_2O_3 and ceria-based solid solution.

Conductivities

Effect of total Mg content

Figure 4 shows the effect of total Mg content (y) on the conductivities of the samples with nominal composition of $Ce_{0.935-y}Y_{0.065}Mg_yO_{1.9675-y}$, wherein $0 \leq y \leq 0.35$, in air and at $873\sim973$ K. The conductivity changed with y like a mountain and at $y =$ about 0.12 reached the maximum of 0.014 S cm^{-1} for 973 K, higher than the value of CGO (0.006 S cm^{-1}), which is

Fig. 4 The effect of total Mg content (y) on the conductivities of the pellet samples with nominal composition of $Ce_{0.935-y}Y_{0.065}Mg_yO_{1.9675-y}$, in air and at 873 K

Fig. 5 SEM micrographs of pellet samples with nominal composition of $Ce_{0.935-y}Y_{0.065}Mg_yO_{1.9675-y}$, **a** $y=0$, **b** $y=0.12$, and **c** $y=0.35$
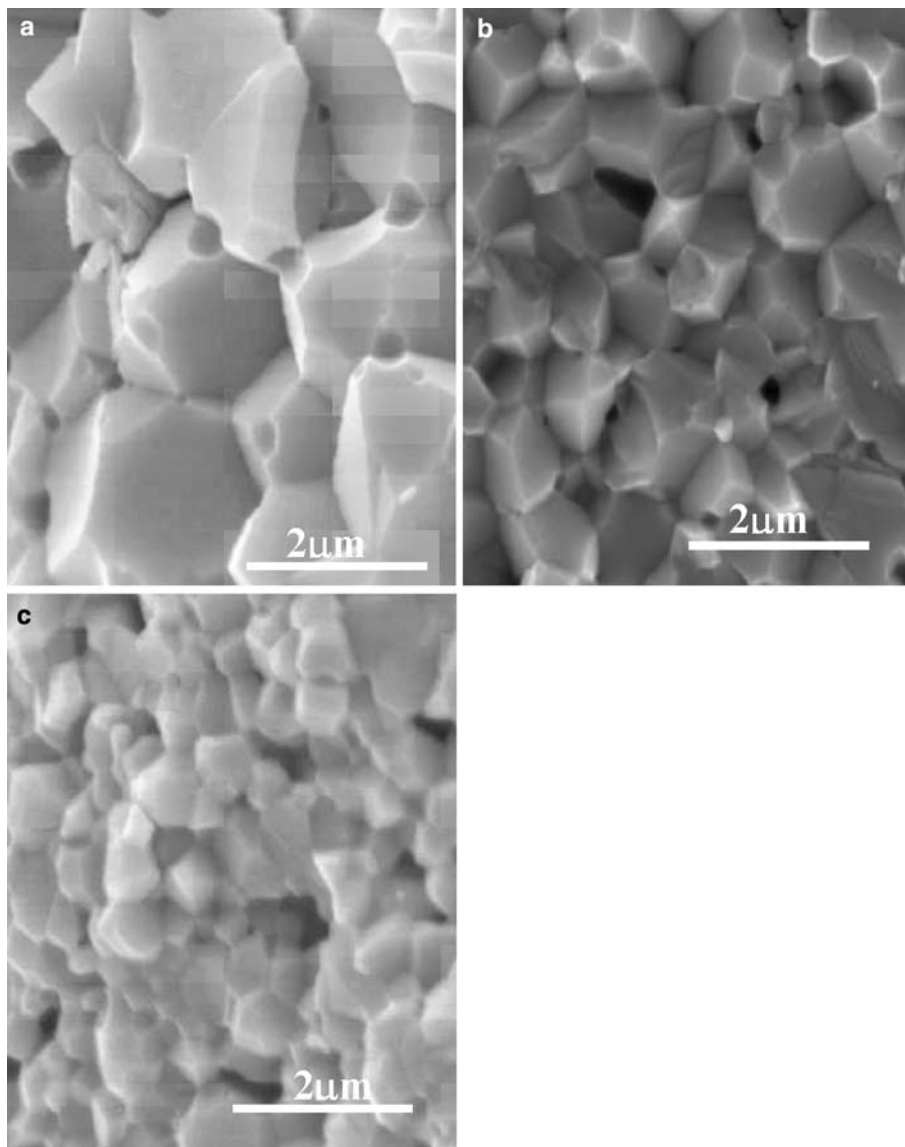

between the values in reference [9] (0.0001 S cm^{-1}) and reference [10] (0.013 S cm^{-1}). Similarly, in the study [11] on Mg doped ceria electrolytes, it was reported that the conductivity at 1,073 K reached its maximum at about 10 mol% of total Mg content. Figure 5 shows the SEM micrographs of representative pellet samples with different total Mg content (y). Apparently, the grain sizes of all the samples are smaller than 3 μm, and decrease with the total Mg content (y) increasing. It has been reported [7] that when the mean grain size of $Ce_{0.8}Gd_{0.2}O_{2-\delta}$ is smaller that 3 μm, both the grain and grain boundary conductivities, especially the latter, increase with grain size decreasing. Analogously, for our results, the decrease of grain size with the increase of total Mg content might cause the increase of total conductivity. On the other hand, the large increase of total Mg content would lead to the large increase of free MgO, which would lead to the decrease of total conductivity because free MgO has much lower con-

ductivity than doped CeO_2. These two opposite effects of total Mg content on conductivity might cause the maximum conductivity emerging at $y=$ about 0.12 (see Fig. 4).

Effect of Y dopant

Figure 6 shows the conductivities in air of the two-phase pellet samples with nominal compositions of $Ce_{0.585}Y_{0.065}Mg_{0.35}O_{1.618}$ and $Ce_{0.65}Mg_{0.35}O_{1.65}$. For comparison, the data of CGO were also included. It can be seen that the existing of dopant Y^{3+} was vital for the samples to have high conductivity, and that the conductivity of the Y-containing sample was close to that of CGO. Similarly, it had been reported that the conductivity of $Ce_{0.9}Y_{0.1}O_{1.95}$ at 1,023 K in air was close to that of CGO [12], and that the conductivity of $Ce_{0.6}Mg_{0.4}O_{1.6}$ was close to that of pure CeO_2 [11].
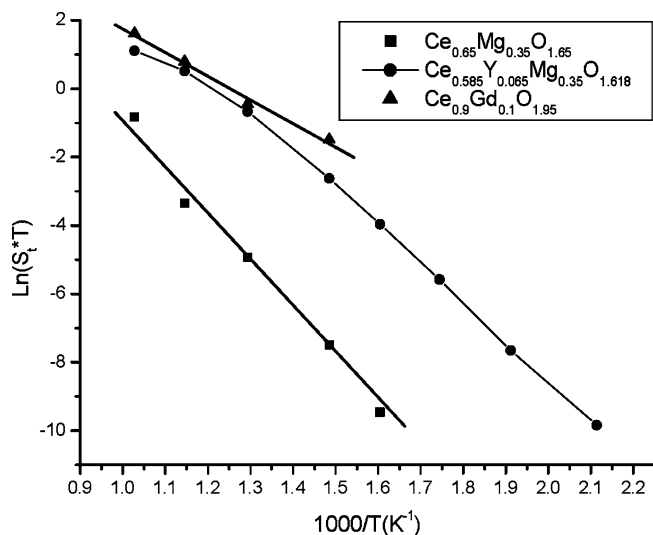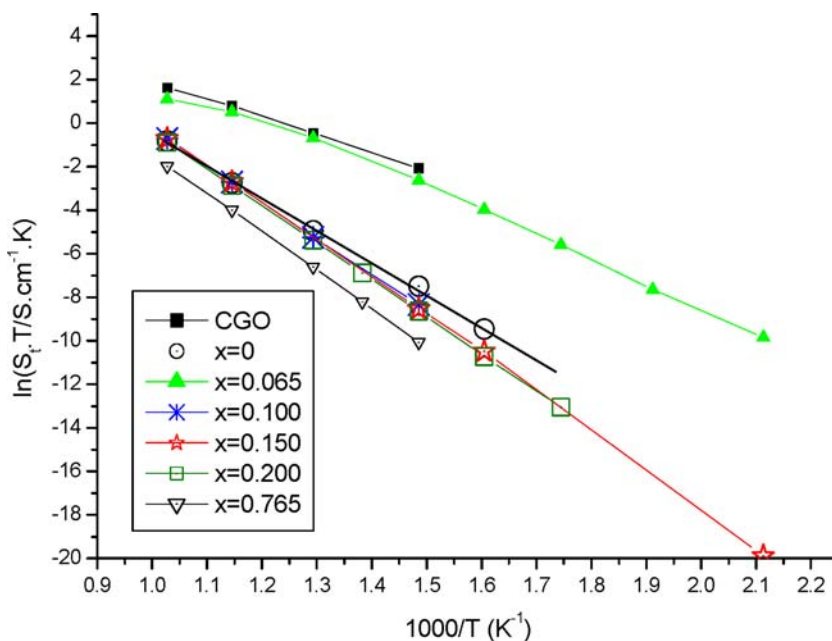
Fig. 6 The effect of temperature on the conductivities of different pellet samples in air with nominal composition of (*square*) $Ce_{0.65}Mg_{0.35}O_{1.65}$, (*circle*) $Ce_{0.585}Y_{0.065}Mg_{0.35}O_{1.618}$, and (*triangle*) CGO

Effect of Y content

In order to investigate the effect of Y content (x) and at the same time to avoid the effect of oxygen content, the conductivities of the pellet samples with the nominal composition of $Ce_{0.618-0.5x}Y_xMg_{0.382-0.5x}O_{1.618}$, wherein $0 \leq x \leq 0.765$, were measured in air and at different temperatures. This experiment was repeated two times, and the relative deviation of conductivity was found less than 5%. The average results were shown in Fig. 7. It can be seen that the sample with $x = 0.065$ was the best, it had lowest activation energy of conduction and the highest conductivity, close to that of CGO. Similarly, it

has been reported that the maximum conductivity of Y^{3+} doped ceria electrolyte at 460 K emerging at the Y content of about 7 mol% [3].

Stability in 10% H_2/N_2

Any changes of an electrolyte sample in structure, composition, valence state etc. will be reflected in its changes in conductivity, therefore, the stability of an electrolyte can be tested by monitoring its conductivity as a function of run time under given conditions. Figure 8 shows the total conductivities (S_t) of pellet samples ($Ce_{0.815}Y_{0.065}Mg_{0.12}O_{2-a}$, CGO, and $Ce_{0.935}Y_{0.065}O_{2-b}$) in 10% H_2/N_2 and at 973 K as a function of run time. The
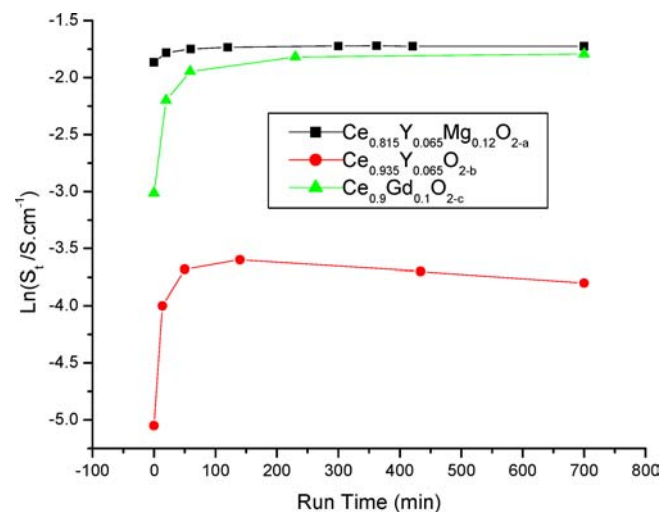
Fig. 8 Changes of total conductivities (S_t) of different pellet samples in 10%H_2/N_2 and at 973 K

Fig. 7 The effect of temperature on the conductivities of CGO and the pellet samples in air with nominal composition of $Ce_{0.618-0.5x}Y_xMg_{0.382-0.5x}O_{1.618}$, wherein $0 \leq x \leq 0.765$

total conductivities of the samples all jumped up when the gas was switched from air to 10% H_2/N_2, then the conductivity quickly approached constant for the first and CGO samples, but decreased considerably with time for the third sample. This result suggests that the existing of MgO benefited the stability of the electrolyte. The same experiment was repeated two times and the relative deviation of conductivity was found less than 8%.

For the sample of $Ce_{0.935}Y_{0.065}O_{2-b}$ in Fig. 8, reduction process proceeded with time continuously. In the first reduction period, a few Ce^{3+} were formed in the ceria lattice, which caused not only the dramatic increase of electronic conductivity, but also a little increase of oxide ion vacancy, and possibly, as a result, a little increase of ionic conductivity. Therefore, the total conductivity increased rapidly and soon reached its maximum. However, with further reduction going on, Ce_2O_3 phase might be formed gradually, which caused the decrease of total conductivity because Ce_2O_3 has much lower conductivity than doped ceria [8].

For the sample of $Ce_{0.815}Y_{0.065}Mg_{0.12}O_{2-a}$ in Fig. 8, MgO exists in two different states. One is as dopant in the ceria lattice, which could not only increase the number of oxide ion vacancy, and consequently increase the ionic conductivity, but also improve the thermodynamic stability of the doped ceria because MgO is much more stable than rare earth oxides especially in reducing environment. Another is free MgO, which is distributed on the crystal surface of the doped ceria. These fine free MgO could, like a cover, decrease the contact area between doped ceria particle surface and reducing gas, and therefore, slow down the reducing process of the doped ceria. In the first period of the reducing process, a few Ce^{3+} were formed in the ceria lattice, which caused a rapid increase of total conductivity, similar to that of $Ce_{0.935}Y_{0.065}O_{2-b}$. However, in the rest period of the reducing process, the co-effect of both MgO might cause the following phenomena. When the sample was reduced to a certain degree before the formation of Ce_2O_3 phase, the system almost approached thermodynamic equilibrium. Therefore, the further reduction of Ce^{4+} approached stop, and the total conductivity of the sample approached constant.

Since MgO is much cheaper than the rare earth oxides, higher content of MgO in the electrolytes also lowers the cost of raw materials of the electrolytes.

Conclusions

Electrolytes with nominal composition of $Ce_{1-x-y}Y_xMg_yO_{2-0.5x-y}$ were prepared and characterized. When $0 \le x \le 0.2$ and $0 \le y \le$ about 0.05, the electrolytes were all single phase materials of ceria-based solid solution. However, when $y >$ about 0.05, the electrolytes became two-phase materials, Y^{3+} and Mg^{2+} co-doped ceria-based solid solution and free MgO. The sample with nominal composition of $Ce_{0.815}Y_{0.065}Mg_{0.12}O_{2-d}$ showed ionic conductivity (0.014 S cm^{-1}) at 973 K close to that of similarly prepared $Ce_{0.9}Gd_{0.1}O_{1.95}$ (CGO), but had lower cost of raw materials and a little higher stability in reducing atmosphere. The existing of free MgO seemed to improve the stability of the electrolytes in reducing atmosphere, but too much free MgO would reduce the conductivity.

References

1. Arai H (1992) J Bull Ceram Soc Jpn 27(2):100
2. Taylor DM, Joshi AV (1995) US Patent 5,378,345
3. Inaba H, Tagawa H (1996) Solid State Ionics 83:1
4. Steele BCH (2000) Solid State Ionics 129:95
5. Maricle DL, Swarr TE, Tuller HL (1991) US Patent 5,001,021
6. Yoshiyuki Maki, Masayuki Matsuda, Tetsuichi Kudo (1971) US Patent 3,607,424
7. Christie GM, van Berkel FPF (1996) Solid State Ionics 83:17
8. Mogensen M, Sammes NM, Tompsett GA (2000) Solid State Ionics 129:63
9. Huang K, Feng M, Goodenough JB (1998) J Am Ceram Soc 81:357
10. Lubke S, Wiemhofer HD (1999) Solid State Ionics 117:229
11. Yahiro H, Ohuchi T, Eguchi K and Arai H (1988) J Mater Sci 23:1036
12. Van Herle J, Horita T, Kawada T, Sakai N, Yokokawa H, Dpkiya M (1996) J Europ Ceram Soc 16:961